perature we expect that the agreement would be somewhat better. (The theory was not calculated for finite temperatures since that would require developing a computer program for the intergals involved and would not add substantially to the general features of the agreement.)

We conclude by observing that the crossing of the curves for zero and nonzero static magnetic field gives strong support to the theory,[3] which attributes the effect of a static magnetic field to the change in kinetic energy of those electrons contributing to the Meissner current in the superconducting penetration depth of the metal. The change in kinetic energy in a field is given by $\mathbf{p} \cdot \mathbf{v} = pv \cos\theta$, where $\mathbf{p}$ is the electron momentum and $\mathbf{v}$ is the drift velocity associated with the Meissner current. As we move around the Fermi surface, $pv \cos\theta$ goes from pv to $-pv$ which effectively introduces anisotropy in the measured excitation spectrum, increasing the absorption at low frequencies and decreasing it at high frequencies.

Finite-Amplitude Helical Mode in Semiconductor Plasmas

Øivin Holter

Institute of Physics, University of Oslo, Oslo, Norway

AND

Roy R. Johnson

Boeing Scientific Research Laboratories, Seattle, Washington

(Received 1 April 1968; revised manuscript received 4 February 1969)

The finite-amplitude helical mode is investigated for a semiconductor plasma. The radial density distribution of the semiconductor plasma column is calculated in the absence of the helical instability. A finite-amplitude helical plasma configuration is superimposed on the steady-state plasma distribution and the conditions for marginal stability are determined. The parameters describing the helical instability are calculated as functions of the amplitude of the superimposed helix. These results are combined with the energy-balance theory for the semiconductor plasma. The wavelength and frequency are calculated as functions of the magnetic field for a constant current in n-InSb.

I. INTRODUCTION

THE helical instability[1,2] is now generally accepted as the origin of the oscillations which develop in a current-carrying semiconductor bar in a sufficiently strong axial magnetic field.[3-7] The helical instability theory was first applied to the explanation of these oscillations by Glicksman,[8] whose results apply to intrinsic material of high injection levels. The thermal background carriers in extrinsic material were incorporated in the theory by Holter,[9] and account for the high frequencies observed in p-InSb.[5] These theories are applicable to impact-ionization plasmas in semiconductors with high surface recombination velocity.

The same basic instability mechanism has been studied in systems with a low surface recombination velocity.[10,11] Hurwitz and McWhorter,[10] in good agreement with their experimental data, could account for oscillations in semiconductors with no injection. Gurevich and Ioffe[11] studied this instability by taking a field-dependent impact ionization into account.

In the gaseous-plasma case, hysteresis effects have been observed,[12-14] the frequency of the finite-amplitude helical oscillations has been measured as a function of the magnetic field[12-16] and the internal paramagnetic field created by the azimuthal current of the helix measured.[17] The onset of an $m = 2$ mode in the presence

[1] B. B. Kadomtsev and A. V. Nedospasov, J. Nucl. Energy **C1**, 230 (1960).

[2] R. R. Johnson and D. A. Jerde, Phys. Fluids **5**, 988 (1962).

[3] I. L. Ivanov and S. M. Ryvkin, Zh. Tekn. Fiz. **28**, 774 (1958) [English transl.: Soviet Phys.—Tech. Phys. **3**, 722 (1958)].

[4] R. D. Larrabee and M. C. Steele, J. Appl. Phys. **31**, 1519 (1960).

[5] B. Ancker-Johnson, in *Proceedings of the Sixth International Conference on the Physics of Semiconductors, Exeter* (The Institute of Physics and the Physical Society, London, 1962), p. 131.

[6] F. Okamoto, T. Koike, and S. Tosima, J. Phys. Soc. Japan **17**, 804 (1962).

[7] T. Misawa and T. Yamada, Japan J. Appl. Phys. **2**, 19 (1963).

[8] M. Glicksman, Phys. Rev. **124**, 1655 (1961).

[9] Ø. Holter, Phys. Rev. **129**, 2548 (1963).

[10] C. E. Hurwitz and A. L. McWhorter, Phys. Rev. **134**, A1033 (1964).

[11] L. E. Gurevich and I. V. Ioffe, Fiz. Tverd. Tela **6**, 445 (1964) [English transl.: Soviet Phys.—Solid State **6**, 354 (1964)].

[12] H. S. Robertson, Phys. Fluids **7**, 1093 (1964).

[13] S. Imazu, Y. Uesaka, T. Sukegawa, and Y. Nakano, J. Phys. Soc. Japan **19**, 418 (1964).

[14] A. A. Zaitsev and B. N. Shvilkin, Radiotekhn. Elektron. **10**, 951 (1965) [English transl.: Radio Eng. Electron. (USSR) **5**, 811 (1965)].

[15] B. E. Cherrington and L. Goldstein, J. Nucl. Energy **C7**, 263 (1965).

[16] A. R. Akhmedov and A. A. Zaitsev, Zh. Tekhn. Fiz. **33**, 177 (1963) [English transl.: Soviet Phys.-Tech. Phys. **8**, 126 (1963)].

[17] R. R. Johnson, in *Proceedings of the Sixth International Conference on Ionization Phenomena in Gases, Paris, 1963* (SERMA, Paris, 1963), Vol. 1, p. 413.

of a finite-amplitude $m=1$ mode has been observed.[15,18] These experimental results are in qualitative agreement with the finite helical-mode theory by Holter and Johnson.[19,20]

The properties of the helical instability of semiconductor plasmas in the finite-amplitude region have been investigated in p-InSb by Ancker-Johnson.[21,22]

In this paper we extend the finite-amplitude helical-mode theory[19] to the semiconductor plasma case. We use the zero- and first-harmonic equations for the density and potential, derived from the equations of motion and continuity. In the zero-harmonic equations we include terms which are nonvanishing when the presence of a finite-amplitude helix is assumed. This then shifts the time-averaged zero-harmonic density profile away from its zero-amplitude appearance. This shift has been shown to be in the predicted direction for the positive column in experiments by Itoh et al.[23] With a modified density profile new conditions for marginal stability are derived by using the first-harmonic equations. The results thus derived are presented in a self-consistent way, although they are not directly applicable to experimental measurements. To facilitate direct comparisons of experimentally measurable quantities for a given material, the results of the stability analysis are combined with an energy-balance analysis. We use a theory, developed by Keldysh[24] and by Chuenkov,[25] which makes possible the calculation of the impact-ionization coefficient, the mobility, and the temperature for a given applied electric field. The analysis presented here neglects the effect of the self-magnetic field of the current; in the Appendix it is shown that this assumption is roughly equivalent to the requirement that the total current be less than 1 A for n-type InSb.

II. BASIC EQUATIONS

We consider a long cylindrical semiconductor bar of radius R with a uniform distribution of thermal background carriers. The semiconductor is situated in an externally created homogeneous axial magnetic field $\mathbf{B}_0$. When an axial electric field E_{z0} is applied, we may get a plasma in the semiconductor either by injection, impact ionization, or both. We assume that the condition of quasineutrality holds and, therefore, we set both the plasma electron and hole densities equal to n.

[18] K. Yatsui and Y. Inuishi, J. Phys. Soc. Japan **22**, 626 (1967).

[19] Ø. Holter and R. R. Johnson, Phys. Fluids **8**, 333 (1965).

[20] Ø. Holter and R. R. Johnson, Phys. Fluids **9**, 622 (1966).

[21] B. Ancker-Johnson, Appl. Phys. Letters **3**, 104 (1963); Phys. Rev. **134**, A1465 (1964).

[22] B. Ancker-Johnson, Phys. Rev. **135**, A1423 (1964); in *Proceedings of the International Symposium on Plasma Effects in Solids* (Dunod Cie., Paris, 1964), p. 165.

[23] S. Itoh, M. Kawaguchi, and K. Yamamoto, Phys. Fluids **9**, 2535 (1966).

[24] L. V. Keldysh, Zh. Eksperim. i Teor. Fiz. **48**, 1962 (1965) [English transl.: Soviet Phys.—JETP **21**, 1135 (1965)].

[25] V. A. Chuenkov, Fiz. Tverd. Tela **9**, 48 (1967) [English transl.: Soviet Phys.—Solid State **9**, 35 (1967)].

The macroscopic equations of motion are

$$\mathbf{\Gamma}_\pm + D_\pm \nabla n \mp \mu_\pm N_\pm \mathbf{E} \mp \mu_\pm \mathbf{\Gamma}_\pm \times \mathbf{B} = 0, \qquad (1)$$

where we have introduced the flow vectors $\mathbf{\Gamma}_\pm = N_\pm \mathbf{v}_\pm$, where $N_\pm$ are the total particle densities $N_\pm = n_\pm + n$, $n_\pm$ are the background carrier densities, and $\mathbf{v}_\pm$ are the velocities. The subscripts $+$ and $-$ refer to holes and electrons, respectively. $D_\pm$ and $\mu_\pm$ are the diffusion coefficients and mobilities, and $\mathbf{B}$ and $\mathbf{E}$ are the total magnetic and electric fields, respectively.

Equations (1) are written down under the assumption that the collision frequency of the electrons and holes with the lattice is much larger than the characteristic frequency of the plasma. Furthermore, the carriers are assumed to be isothermal.

The continuity equations are

$$\partial n / \partial t + \nabla \mathbf{\Gamma} = \xi_+ N_+ + \xi_- N_- - n/\tau, \qquad (2)$$

where $\xi_\pm$ are the number of electron-hole pairs created per second per hole and electron, respectively, and τ is the average bulk lifetime of injected carriers.

The explicit expressions for $\mathbf{\Gamma}_\pm$ are obtained from Eqs. (1):

$$\mathbf{\Gamma}_\pm = -D_\pm' \nabla n \pm \mu_\pm' N_\pm \mathbf{E} \pm \mu_\pm D_\pm' \mathbf{B} \times \nabla n$$
$$-\mu_\pm' \mu_\pm N_\pm \mathbf{B} \times \mathbf{E} - \mu_\pm^2 D_\pm' \mathbf{B}(\mathbf{B} \cdot \nabla n)$$
$$\pm \mu_\pm' \mu_\pm^2 N_\pm \mathbf{B}(\mathbf{B} \cdot \mathbf{E}), \qquad (3)$$

where we have introduced

$$\mu_\pm' = \frac{\mu_\pm}{1 + \mu_\pm^2 B^2}, \quad D_\pm' = \frac{D_\pm}{1 + \mu_\pm^2 B^2}. \qquad (4)$$

We eliminate $\mathbf{\Gamma}_\pm$ between Eqs. (2) and (3) and obtain in cylindrical coordinates

$$\xi_+ N_+ + \xi_- N_- - \frac{n}{\tau} - \frac{\partial n}{\partial t} + D_\pm' \left[\frac{1}{r} \frac{\partial}{\partial r} \left(r \frac{\partial n}{\partial r} \right) + \frac{1}{r^2} \frac{\partial^2 n}{\partial \theta^2} \right]$$

$$\pm \mu_\pm \left[\frac{1}{r} \frac{\partial}{\partial r} \left(r N_\pm \frac{\partial U}{\partial r} \right) + \frac{1}{r^2} \frac{\partial}{\partial \theta} \left(N_\pm \frac{\partial U}{\partial \theta} \right) \right]$$

$$-\mu_\pm' \mu_\pm B_0 \frac{1}{r} \left(\frac{\partial n}{\partial \theta} \frac{\partial U}{\partial r} - \frac{\partial n}{\partial r} \frac{\partial U}{\partial \theta} \right) + D_\pm \frac{\partial^2 n}{\partial z^2}$$

$$\pm \mu_\pm \frac{\partial}{\partial z} \left(N_\pm \frac{\partial U}{\partial z} \right) = 0, \qquad (5)$$

where U is the electric potential. We have assumed the magnetic field to be the applied magnetic field only, i.e., $\mathbf{B} = \mathbf{B}_0$, thus neglecting the internal field. The temperatures $V_\pm$ are expressed in electron volts and are introduced through the Einstein relations $D_\pm = \mu_\pm V_\pm$.

III. HELICAL-MODE TREATMENT

We assume that in the unperturbed steady state there are no variations in the z direction of the electric

field and plasma density. A perturbation analysis of the steady-state system has previously been performed.[9] This analysis shall now be extended to the finite-amplitude case by employing the method developed for treating the finite-amplitude helical mode in the positive column.[19] We postulate the existence of a finite-amplitude helix superimposed on a stationary background plasma. We first analyze the functional form of the zero-order stationary plasma, which is constituted by the thermal background plasma together with the unperturbed steady-state plasma modified by the presence of the finite-amplitude helix. Then the stationary density profile is used in the calculations of the stability of the helix. We assume that we have a

uniform applied electric field E_{z0} present. As an approximation, we shall only consider the first harmonic of the helical mode. For this case we shall express the plasma density and plasma potential as

$$n = \mathrm{Re}\{N_0 h_0(r) + N_1 f(r) \exp[i(\omega t + kz + m\theta)]\}, \quad (6)$$

$$U = \mathrm{Re}\{U_0(r) - E_{z0}z + U_1 g(r) \\ \times \exp[i(\omega t + kz + m\theta + \delta)]\}, \quad (7)$$

where k, m, δ, N_1, U_1, and N_0 are real constants, h_0, U_0, f, and g are real functions of r, and $\omega = \omega_r + i\omega_i$ is complex.

We substitute these expressions into Eqs. (5) and consider the case where $\omega_i t \ll 1$; we get

$$\xi_- n_- + \xi_+ n_+ + \left(\xi_- + \xi_+ - \frac{1}{\tau}\right) N_0 h_0 + D_{\pm}' N_0 \frac{1}{r} \frac{d}{dr}\left(r \frac{dh_0}{dr}\right) \pm \mu_{\pm}' \frac{1}{r} \frac{d}{dr}\left(r(n_{\pm} + N_0 h_0)\frac{dU_0}{dr}\right)$$

$$\pm \mu_{\pm}' \frac{1}{r} \frac{d}{dr}\left(rf\frac{dg}{dr}\right) \tfrac{1}{2} N_1 U_1 \cos\delta - \mu_{\pm}' \mu_{\pm} B_0 \frac{m}{r} \frac{d}{dr}(fg)\tfrac{1}{2} N_1 U_1 \sin\delta$$

$$+ \mathrm{Re}\left(\left\{\left(\xi_- + \xi_+ - \frac{1}{\tau} - i\omega\right)f + D_{\pm}'\left[\frac{1}{r}\frac{d}{dr}\left(r\frac{df}{dr}\right) - \frac{m^2}{r^2}f\right] - k^2 D_{\pm} f - \frac{im}{r}\mu_{\pm}' \mu_{\pm} B_0 f \frac{dU_0}{dr}\right.\right.$$

$$\left. \pm \mu_{\pm}' \frac{1}{r}\frac{d}{dr}\left(rf\frac{dU_0}{dr}\right) \mp i\mu_{\pm} kf E_{z0}\right\} N_1 \exp[i(\omega t + kz + m\theta)]$$

$$+ \left\{\pm \mu_{\pm}'\left[\frac{1}{r}\frac{d}{dr}\left(r(n_{\pm} + N_0 h_0)\frac{dg}{dr}\right) - \frac{m^2}{r^2}(n_{\pm} + N_0 h_0)g\right]\right.$$

$$\left.\left. \mp \mu_{\pm}(n_{\pm} + N_0 h_0)k^2 g + \frac{im}{r}\mu_{\pm}' \mu_{\pm} B_0 N_0 g \frac{dh_0}{dr}\right\} U_1 \exp[i(\omega t + kz + m\theta + \delta)]\right) = 0. \quad (8)$$

The constant m is retained in these equations for possible consideration of other modes, but for the treatment presented here we shall set $m = 1$ for all the numerical calculations. We do not attempt to incorporate effects due to second harmonics, and we have retained only the zero- and first-harmonic terms in these equations. The coefficients in front of the exponential terms are independent of time and each coefficient must be equal to zero. Equations (8), therefore, split into four equations. First we consider the two zero-harmonic equations.

IV. ZERO-HARMONIC EQUATIONS

From the zero-harmonic portions of Eqs. (8), we first derive

$$\frac{dU_0}{dr} = \frac{V_- + V_+}{2\eta_2(h_0 + \gamma)}\left[-C_1\frac{dh_0}{dr} + C_2\left(\psi\frac{dg}{dr} + \phi\frac{g}{r}\right)f\right], \quad (9)$$

where we have integrated once, noting that the constant

of integration must equal zero for a regular solution, and introduced the appropriate definitions from Table I.

Using Eq. (9) to eliminate U_0, we derive the following equation for h_0:

$$\frac{1}{r}\frac{d}{dr}r\frac{dh_0}{dr} + C_1\frac{1}{r}\frac{d}{dr}\left(\frac{r}{h_0 + \gamma}\frac{dh_0}{dr}\right)$$

$$- \frac{1}{r}\frac{d}{dr}\left[\phi\left(1 + \frac{C_2}{h_0 + \gamma}\right)fg + \psi\frac{C_2}{h_0 + \gamma}rf\frac{dg}{dr}\right]$$

$$+ \beta_0^2(h_0 + \gamma_z) = 0. \quad (10)$$

For the integration over f and g we need to know their radial dependences only since amplitude factors are included in N_1 and U_1. Since we are unable to find the solutions $f(r)$ and $g(r)$, we use trial functions for the radial dependences. In a first approximation we obtain from the linear theory[9]

$$f(r) = J_m(\beta_1 r), \quad g(r) = J_m(\beta_1 r)/(h_0 + \gamma), \quad (11)$$

with the boundary conditions

$$f(0)=g(0)=f(R)=g(R)=0, \quad (12)$$

where we have assumed an infinite surface recombination velocity s_R, and, therefore, set the density at $r=R$ equal to zero.

We make the substitutions for $f(r)$ and $g(r)$ in Eq. (10) and integrate twice to obtain

$$h_0(x)-1+C_1\ln\left(\frac{h_0(x)+\gamma}{1+\gamma}\right)-\tfrac{1}{2}C_2\psi\left(\frac{J_m[(\beta_1/\beta_0)x]}{h_0(x)+\gamma}\right)^2$$
$$-\phi\int_0^x\frac{1}{x'}\left(1+\frac{C_2}{h_0(x')+\gamma}\right)\frac{J_m{}^2[(\beta_1/\beta_0)x']}{h_0(x')+\gamma}dx'$$
$$+\int_0^x x'\ln\left(\frac{x}{x'}\right)[h_0(x')+\gamma_z]dx'=0, \quad (13)$$

where we have employed the boundary condition $h_0(0)=1$ and have put $x=\beta_0 r$.

With $h_0(\beta_0 R)=J_m(\beta_1 R)=0$ we obtain the relation for $\beta_0 R$ in terms of ϕ and ψ [implicit through $h_0(x)$]:

$$1+C_1\ln\left(1+\frac{1}{\gamma}\right)$$
$$-\int_0^{\beta_0 R}x'\ln\left(\frac{\beta_0 R}{x'}\right)h_0(x')dx'-\gamma_z(\beta_0 R/2)^2$$
$$+\phi\int_0^{\beta_0 R}\frac{1}{x'}\left(1+\frac{C_2}{h_0(x')+\gamma}\right)\frac{J_m{}^2[(\beta_1/\beta_0)x']}{h_0(x')+\gamma}dx'=0. \quad (14)$$

We shall designate $\beta_{00}R$ to be determined from the zero-amplitude equation and define $\Delta\beta_0 R=\beta_0 R-\beta_{00}R$.

Equation (13) reveals a significant difference between extrinsic and intrinsic material (and a gaseous plasma). For the intrinsic case $C_2=0$, and the equation for h_0 is independent of ψ. For this case we may specify ϕ, which determines the zero-order solution used in the stability analysis. The dispersion relation obtained from the first-harmonic equations is then used to calculate ψ for the given ϕ value. For extrinsic material, however, we are not free to choose both ϕ and ψ since they are connected by an equation obtained from the first-harmonic equations (see Sec. V). Thus, we shall have to solve a considerably more complex numerical problem for this case, namely, the simultaneous solution of the zero- and first-harmonic equations.

TABLE I. Definitions used in the derivations.

$$b=\mu_-/\mu_+, \quad b_v=V_-/V_+, \quad b_z=\xi_+/\xi_-$$
$$\gamma_3=(b-1)/\sqrt{b}, \quad \gamma_5=(b+1)/\sqrt{b}, \quad \gamma_6=\frac{b_v-1}{b_v+1}, \quad \gamma_7=\frac{1-b_z}{1+b_z}$$
$$\eta_1=\tfrac{1}{2}(n_-+n_+)/N_0, \quad \eta_2=\tfrac{1}{2}(n_--n_+)/N_0$$
$$y=\mu_-\mu_+B_0{}^2, \quad a_7=\gamma_3 y^{1/2}/(1+y)$$
$$\beta_0{}^2=(1/\mu_-)(b+1)(1+y)(\xi_-+\xi_+-1/\tau)/(V_-+V_+),$$
$$C_{01}=1-(\beta_0/\beta_1)^2$$
$$\phi=\tfrac{1}{2}m(\mu_-+\mu_+)B_0\sin\delta\frac{N_1U_1}{N_0(V_-+V_+)}, \quad \psi=-\frac{a_7}{m}\phi\cot\delta$$
$$\gamma=\eta_1+\eta_2\frac{\gamma_3}{\gamma_5}\frac{1-y}{1+y},$$
$$\gamma_z=(\eta_1+\eta_2\gamma_7)\left(1+(b+1)(1+y)\frac{1/\tau}{\mu_-(V_-+V_+)\beta_0{}^2}\right)$$
$$C_1=-\eta_2\left(\gamma_6+\frac{\gamma_3}{\gamma_5}\frac{1-y}{1+y}\right), \quad C_2=-n_2\frac{2\gamma_3}{\gamma_5(1+y)}$$
$$b_{11}=(b+1)(1+y)(\beta_1 R)^{-2}[\omega_r R^2/\mu_-(V_-+V_+)]$$
$$b_{21}=(b+1)(1+y)(\beta_1 R)^{-2}[\omega_i R^2/\mu_-(V_-+V_+)]$$
$$x_1=\frac{k}{\beta_1}=\frac{2\pi}{\beta_1 R}\frac{R}{\lambda}, \quad z_1=(1+y)x_1{}^2, \quad b_{31}=\frac{E_{z0}R}{\beta_1 R(V_-+V_+)}$$

For the purpose of numerical calculations we shall restrict the analysis to the case where $s_R=\tau=\infty$, corresponding to the boundary condition $h_0(R)=0$ on the plasma density, and an infinite bulk lifetime of the injected carriers. In Fig. 1 we have plotted h_0 as a function of η_1 and η_2 for the zero-amplitude case, which does not require the use of the first-harmonic equations. In Fig. 2 we have plotted the quantity $\beta_{00}R$ as a function of η_1 and η_2 for the zero-amplitude case.

V. FIRST-HARMONIC EQUATIONS

We shall use the first-harmonic equations to derive the conditions for stability of a finite-amplitude helix. We drop the real notation and the exponential term in Eqs. (8) and set the first-harmonic terms equal to zero. We then rewrite these equations in terms of a new function $l(r)$ which satisfies Bessel's equation:

$$l(r)=g(r)(h_0+\gamma)+\frac{C_1(V_-+V_+)}{2\eta_2}\frac{N_1}{N_0U_1}e^{i\delta}f(r). \quad (15)$$

We make the substitutions for $l(r)$ and dU_0/dr, and obtain

$$\left\{\left(\frac{\mu_-\mu_+(V_-+V_+)}{(1+y)(\mu_-+\mu_+)}\right)\left[\frac{1}{r}\frac{d}{dr}\left(r\frac{df}{dr}\right)-\frac{m^2}{r^2}f-\frac{\mu_\pm}{\mu_\pm{}'}k^2f\right]+\left[\xi_-+\xi_+-\frac{1}{\tau}-i\omega\mp i\mu_\pm kE_{z0}\right]f\right\}N_1$$
$$+\left(\pm\mu_\pm{}'\left\{\frac{1}{r}\frac{d}{dr}\left[r\left(\psi\frac{dg}{dr}+\phi\frac{g}{r}\right)fg\right]\right\}-\frac{im}{r}\mu_\pm{}'\mu_\pm B_0\left(\psi\frac{dg}{dr}+\phi\frac{g}{r}\right)fg\right)\frac{N_1(V_-+V_+)C_2}{2\eta_2}$$
$$+\left\{\pm\mu_\pm{}'\left[\frac{1}{r}\frac{d}{dr}\left(r\frac{dl}{dr}\right)-\frac{m^2}{r^2}l-\frac{1}{r}\frac{d}{dr}\left(r\frac{l}{h_0+\gamma}\frac{dh_0}{dr}\right)\right]\mp\mu_\pm k^2l+\frac{im}{r}\mu_\pm{}'\mu_\pm B_0\frac{l}{h_0+\gamma}\frac{dh_0}{dr}\right\}N_0U_1e^{i\delta}$$
$$\pm\left\{\mu_\pm{}'\left[\frac{1}{r}\frac{d}{dr}\left(r\frac{dg}{dr}\right)-\frac{m^2}{r^2}g\right]-\mu_\pm k^2g\right\}(n_\pm-\gamma N_0)U_1e^{i\delta}=0. \quad (16)$$
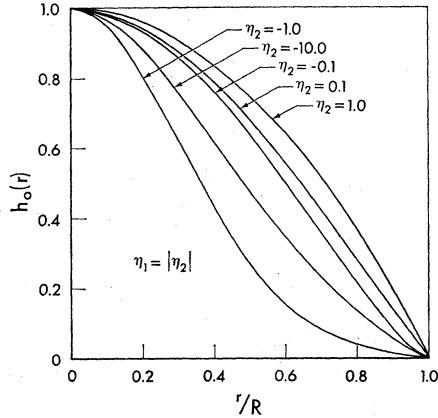
FIG. 1. Unperturbed steady-state plasma density profile for different values of η_1 and η_2, with $y=10^{-4}$, $b=62.5$, $b_z=0$, and $b_v=1$.

We multiply these equations with $\beta_1{}^2 r J_m(\beta_1 r)dr$, integrate from zero to R, and introduce the transformed quantities $F(\beta_1)$ and $L(\beta_1)$,

$$F(\beta_1) = \int_0^R \beta_1{}^2 r f J_m(\beta_1 r)dr$$

$$= -\int_0^R r\left[\frac{1}{r}\frac{d}{dr}\left(r\frac{df}{dr}\right) - \frac{m^2}{r^2}f\right]J_m(\beta_1 r)dr, \quad (17)$$

$$L(\beta_1) = \left(1 - \frac{C_1}{2\eta_2}\frac{N_1(V_-+V_+)}{N_0 U_1}e^{-i\delta}\right)F(\beta_1), \quad (18)$$

and the following integrals:

$$A_{11}L(\beta_1) = -m\int_0^R \frac{l}{h_0+\gamma}\frac{dh_0}{dr}J_m(\beta_1 r)dr,$$

$$D_{11}L(\beta_1) = L(\beta_1) + \int_0^R \frac{d}{dr}\left(r\frac{l}{h_0+\gamma}\frac{dh_0}{dr}\right)J_m(\beta_1 r)dr,$$

$$W_{11}L(\beta_1) = \int_0^R \beta_1{}^2 r\frac{l}{h_0+\gamma}J_m(\beta_1 r)dr,$$

$$F_{11}F(\beta_1) = \int_0^R \frac{d}{dr}\left(r\frac{f^2}{h_0+\gamma}\frac{dg}{dr}\right)J_m(\beta_1 r)dr, \quad (19)$$

$$G_{11}F(\beta_1) = \int_0^R \frac{d}{dr}\left(\frac{f^2 g}{h_0+\gamma}\right)J_m(\beta_1 r)dr,$$

$$H_{11}F(\beta_1) = m\int_0^R \frac{f^2}{h_0+\gamma}\frac{dg}{dr}J_m(\beta_1 r)dr,$$

$$P_{11}F(\beta_1) = m\int_0^R \frac{1}{r}\frac{f^2 g}{h_0+\gamma}J_m(\beta_1 r)dr,$$

where $\beta_1 R$ is the first zero of $J_m(\beta_1 r)$ which for $m=1$ has the value 3.8317. By noting that

$$\frac{N_0 U_1}{N_1(V_-+V_+)}e^{i\delta} = \left(\frac{N_0}{N_1}\right)^2\frac{2\gamma_3}{\gamma_5(1+y)}\left(\psi + i\frac{\phi}{ma_7}\right), \quad (20)$$

and using the definitions of Table I, we derive the following two equations:

$$(C_{01}+ib_{11}-b_{21})[D_{11}-ia_7 A_{11}+(1-yC_2 W_{11})(1+a_7{}^2)z_1]$$
$$-i(\sqrt{z_1})(b_{31}\gamma_5/\gamma_3)(1+y)^{3/2}[a_7{}^2 D_{11}+ia_7 A_{11}+C_2 W_{11}(1+a_7{}^2)(1+z_1)]$$
$$+z_1[(1+ya_7{}^2)D_{11}+(1+a_7{}^2)z_1-ia_7 A_{11}(1-y)+yC_2 W_{11}(1+a_7{}^2)]$$
$$+[\psi F_{11}+\phi G_{11}][a_7{}^2 z_1 - ia_7 A_{11}-C_2 W_{11}(1+(1+ya_7{}^2)z_1)]$$
$$-ia_7[\psi H_{11}+\phi P_{11}][D_{11}+z_1+C_2 W_{11}(1+(1-y)z_1)]$$
$$+C_2 W_{11}[D_{11}(1+(1+ya_7{}^2)z_1)+(1+a_7{}^2)z_1(1+z_1)-ia_7 A_{11}(1+(1-y)z_1)]]=0, \quad (21)$$

$$C_{01}+ib_{11}-b_{21}+\phi G_{11}+\psi F_{11}+i(\sqrt{z_1})(\gamma_5/\gamma_3)b_{31}(1+y)^{3/2}+z_1(1-y)$$
$$-(D_{11}+z_1)C_1/C_2+[D_{11}+z_1+C_2 W_{11}(1+(1-y)z_1)][(2N_0{}^2/N_1{}^2)(\psi+i\phi/ma_7)]=0. \quad (22)$$

Before deriving the dispersion relation, and subsequently the conditions for stability, let us inspect our system of equations. Equations (20), (21) and (22), with their real and imaginary parts, constitute a set of six equations. With Eqs. (13) and (14), we then have available eight equations. In these equations a total of 17 unknown quantities are included: z_1, b_{31}, b_{21}, b_{11}, ϕ, ψ, h_0, N_0/N_1, $\mu_1/(V_-+V_+)$, δ, y, $\beta_0 R$, μ_-/μ_+, $b_z b_v$, η_1, and η_2. We are primarily interested in calculating the dimensionless wavelength λ/R, the dimensionless electric field $E_{z0}R/(V_-+V_+)$, and the dimensionless fre-

quency $\omega_r R^2/\mu_-(V_-+V_+)$ as functions of the dimensionless magnetic field $\mu_-\mu_+ B_0{}^2$. Using Table I, we see that this amounts to solving our equations for z_1, b_{31}, and b_{11} as functions of y. With the conditions for marginal stability we have $b_{21}=0$, and the condition $db_{21}/dz_1=0$, to give us a total of nine equations. Of the unknowns, the ratios b, b_z, and b_v, together with η_1 and η_2, may be estimated from the semiconductor material and the experimental conditions. That leaves us with a total of 11 unknowns, two of which must be specified, for instance, y and $\beta_0 R$.
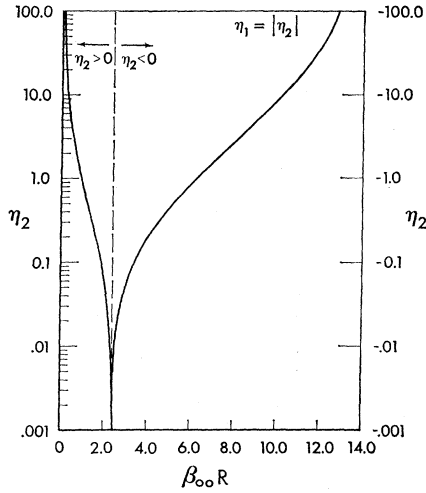
Ø. HOLTER AND R. R. JOHNSON

FIG. 2. Argument $\beta_{00}R$ for the unperturbed plasma density plotted as a function of η_1 and η_2, with $y=10^{-4}$, $b=62.5$, $b_z=0$, and $b_v=1$.

VI. THE DISPERSION RELATION

First we derive an equation between ϕ and ψ from which $\cot\delta$ can be obtained. We write out the real and imaginary components of Eq. (22) and then eliminate $(N_0/N_1)^2$ from the resulting equations. We thus obtain

$$\phi[C_{01}-b_{21}+\phi G_{11}+\psi F_{11}+(1-y)z_1-(C_1/C_2)(D_{11}+z_1)]$$
$$= ma_7\psi[b_{11}+(\sqrt{z_1})(\gamma_5/\gamma_3)b_{31}(1+y)^{3/2}], \quad (23)$$

from which $\cot\delta$ can be calculated by using Eq. (20).

TABLE II. Definitions used in the derivations.

$A = a_7A_{11}[D_{11}+z_1+(1+(1-y)z_1)C_2W_{11}]$

$B = [D_{11}+z_1+(1+(1-y)z_1)C_2W_{11}]^2$

$C = [D_{11}+(1+a_7^2)(1-yC_2W_{11})z_1]$
$\qquad \times [D_{11}+z_1+(1+(1-y)z_1)C_2W_{11}]$

$D = [D_{11}+(1+a_7^2)(1-yC_2W_{11})z_1]^2+a_7^2A_{11}^2$

$E = b_{31}(1+y)^{3/2}\gamma_5/\gamma_3$

$V = y(1+a_7^2)(1+C_1W_{11})z_1$

$G = C_{01}+C_1W_{11}-b_{21}+(1-y)(1+C_1W_{11})z_1$

$\Gamma_1 = (D-C)F_{11}+a_7AH_{11}$	$\Gamma_7 = a_7AH_{11}-CF_{11}$
$\Gamma_2 = a_7BH_{11}+AF_{11}$	$\Gamma_{11} = \Gamma_5\Gamma_3-\Gamma_1\Gamma_7/ma_7$
$\Gamma_3 = a_7CH_{11}+AF_{11}$	$\Gamma_{12} = (B-C)\Gamma_5+A\Gamma_1/ma_7$
$\Gamma_4 = a_7[F_{11}P_{11}-G_{11}H_{11}]$	$\Gamma_{13} = \Gamma_5\Gamma_2+CF_{11}\Gamma_1/ma_7$
$\Gamma_5 = (D-C)G_{11}+a_7AP_{11}$	$\Gamma_{14} = DG+CV$

$\Gamma_6 = a_7CP_{11}+AG_{11}$

$a_0 = Az_1(1+a_7^2)^2F_{11}(B-C)$

$b_0 = [F_{11}(B-C)\Gamma_{14}$
$\qquad +A(\Gamma_3G+\Gamma_2V+\phi(B-C)\Gamma_4)+\phi F_{11}\Gamma_{12}]z_1^{1/2}(1+a_7^2)$

$c_0 = \Gamma_{14}[\Gamma_3G+\Gamma_2V+\phi(B-C)\Gamma_4]$
$\qquad +\phi\left[G\Gamma_{11}+V\Gamma_{13}+\phi\Gamma_4\Gamma_{12}+\Gamma_1^2B^{1/2}\dfrac{\gamma_5\sqrt{y}}{2ma_7^2}\left(\gamma_6+\dfrac{\gamma_3}{\gamma_5}\dfrac{1-y}{1+y}\right)\right]$

We write out the real and imaginary components of Eq. (21), which we obtain after multiplying the equation by $D_{11}+(1+a_7^2)z_1+ia_7A_{11}-yC_2W_{11}(1+a_7^2)z_1$. The resulting equations are

$$[b_{11}+(\sqrt{z_1})E]D-(\sqrt{z_1})EC(1+a_7^2)$$
$$-A(\psi F_{11}+\phi G_{11})-a_7C(\psi H_{11}+\phi P_{11})$$
$$+(1+C_2W_{11})Ayz_1(1+a_7^2)=0, \quad (24)$$

$$[C_{01}+C_2W_{11}-b_{21}+\psi F_{11}+\phi G_{11}+(1-y)(1+C_2W_{11})z_1]D$$
$$+(\sqrt{z_1})E(1+a_7^2)A$$
$$-C[\phi F_{11}+\phi G_{11}-y(1+a_7^2)(1+C_2W_{11})z_1]$$
$$+a_7A(\psi H_{11}+\phi P_{11})=0, \quad (25)$$

where the definitions of Table II are employed.

We eliminate $b_{11}+(\sqrt{z_1})E$ and ψ between Eqs. (23)–(25) and obtain an equation which can be written in the simplified form

$$a_0E^2+b_0E+c_0=0, \quad (26)$$

where the coefficients a_0, b_0, and c_0, given in Table II, are functions of the magnetic field and wavelength of the helix. The quantity E represents the longitudinal electric field which occurs in the electron-hole plasma. We eliminate the quantity E from Eq. (31) by imposing the condition of marginal stability which selects the wavelength of the helix that is most unstable.

If in Eq. (26) we let the electric field increase, while the other quantities, except b_{21} and z_1, remain fixed, the growth rate will eventually become positive for some value of z_1. At this point of marginal stability the derivative of Eq. (26) with respect to z_1 will be zero. Dividing by the quantity a_0 and differentiating, we then obtain

$$\left[2z_1\frac{d}{dz_1}\left(\frac{b_0}{a_0}\right)-\frac{b_0}{a_0}\right]E+2\left[z_1\frac{d}{dz_1}\left(\frac{c_0}{a_0}\right)-\frac{c_0}{a_0}\right]=0, \quad (27)$$
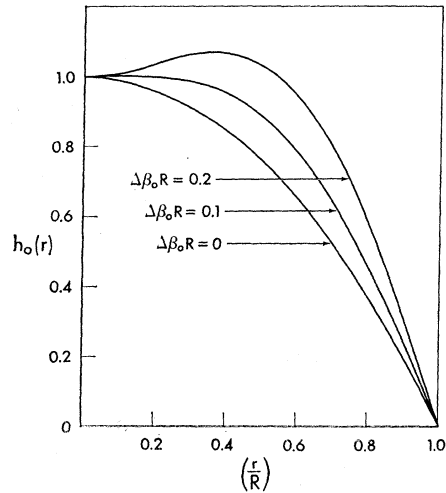

FIG. 3. Zero-harmonic plasma density profile for different values of ϕ, with $\eta_1=\eta_2=1$, $y=10^{-4}$, $b=62.5$, $b_z=0$, and $b_v=1$.

which, when used to eliminate E in Eq. (26), yields the equation for z_1:

$$4\left[z_1\frac{d}{dz_1}\left(\frac{a_0}{c_0}\right)+\frac{a_0}{c_0}\right]^2-\left(\frac{b_0}{c_0}\right)^2\left[2z_1\frac{d}{dz_1}\left(\frac{a_0}{b_0}\right)+\frac{a_0}{b_0}\right]$$

$$\times\left[2z_1\frac{d}{dz_1}\left(\frac{b_0}{c_0}\right)+\frac{b_0}{c_0}\right]=0. \quad (28)$$

By inspection of the coefficients a_0, b_0, and c_0 we find that, in addition to z_1, they include the following seven unspecified quantities: y, μ_-/μ_+, V_-/V_+, η_1, η_2, β_0R, h_0, and ϕ. To solve for z_1, we may specify the mobility ratio μ_-/μ_+, the temperature ratio V_-/V_+, and the density ratios n_+/N_0 and n_-/N_0 which enter into η_1 and η_2. We could then compute z_1 as a function of y for different values of the amplitude parameter ϕ. To do this, however, we have to calculate β_0R and $h_0(r)$, which enter into the integrals Eq. (19), for the same parameters. Equations (13) and (14) for h_0 and β_0R also depend on the additional parameters b_z and ψ. The ratio $b_z=\xi_+/\xi_-$ may be specified, but ψ has to be computed from Eq. (23). Thus, with the proper specification of the above quantities, we have the four equations (13), (14), (23), and (28), which we solve for $h_0(r)$, β_0R, ψ, and z_1 as functions of y for different values of ϕ.

In Fig. 3 we plot the zero-harmonic density profile as a function of $\Delta\beta_0R$, which is the increase in the value of β_0R from its zero-amplitude value $\beta_{00}R$. In Fig. 4 we plot the dimensionless wavelength λ/R as function of the magnetic field y for various values of $\Delta\beta_0R$.

When z_1 has been determined, we obtain E from Eq. (27), and b_{11} can then be calculated from Eq. (24). Then, using Tables I and II, we calculate the dimensionless electric field $E_{z0}R/(V_-+V_+)$ and frequency $\omega_rR^2/(V_-+V_+)\mu_-$. Finally, we obtain N_1/N_0 from Eq. (22) and $U_1/(V_-+V_+)$ from

$$\frac{U_1}{V_-+V_+}=\frac{2\gamma_3}{(1+y)\gamma_5}\left[\psi^2+\left(\frac{\phi}{ma_7}\right)^2\right]^{1/2}\frac{N_0}{N_1}, \quad (29)$$

obtained by combining the real and imaginary parts of

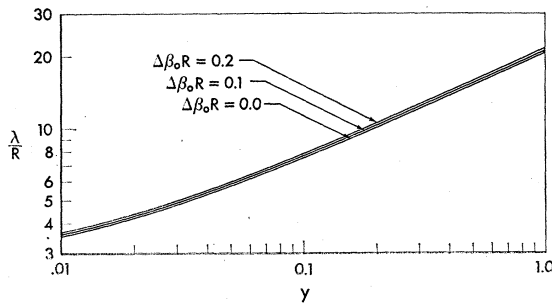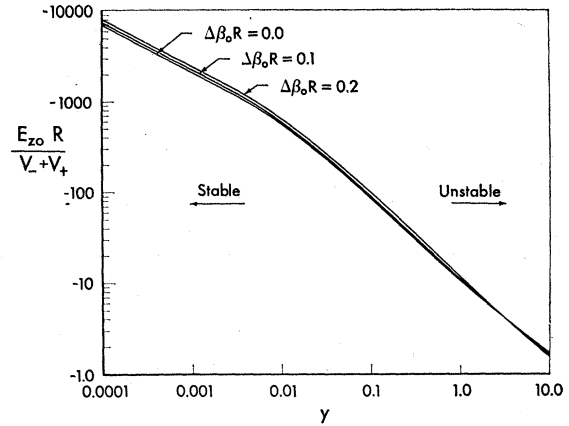FIG. 5. Dimensionless electric field $E_{z0}R/(V_-+V_+)$ as a function of y for various values of $\Delta\beta_0R$ with $\eta_1=\eta_2=1$, $b=62.5$, $b_z=0$, and $b_v=1$.

Eq. (20). In Figs. 5 and 6 we plot $E_{z0}R/(V_-+V_+)$ and $\omega_rR^2/\mu_-(V_-+V_+)$ as a function of y for various values of $\Delta\beta_0R$.

We note that, for the case of a field-dependent ionization coefficient to be considered in Sec. VIII, the quantities b_0 and c_0 will be functions of the electric field through $(\beta_0R)^2$, which enters into G. For that case we then must solve Eqs. (27) and (28) simultaneously for the two unknowns E and z_1. This may be done either numerically or by a graphical technique. In our applications we shall use the former method.

The zero of h_0, β_0R, is obtained from the solution of Eq. (14). For each value of β_0R we calculate from the stability equations a corresponding value for the electric field. When ϕ increases, β_0R increases, corresponding to an increased radial particle flux, which, in order to maintain equilibrium, must be compensated by a corresponding increase in ionization in the bulk. In order to ensure this balance, the stability calculations must be combined with a relation between β_0R and E_{z0}.
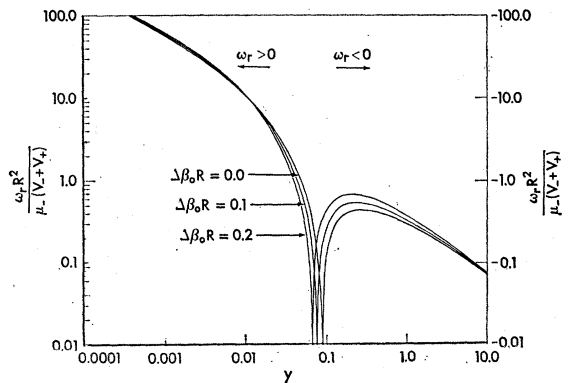

FIG. 4. Dimensionless wavelength λ/R as a function of the magnetic field for various values of $\Delta\beta_0R$, with $\eta_1=\eta_2=1$, $b=62.5$, $b_z=0$, and $b_v=1$.

FIG. 6. Dimensionless frequency $\omega_rR^2/\mu_-(V_-+V_+)$ as a function of y for various values of $\Delta\beta_0R$, with $\eta_1=\eta_2=1$, $b=62.5$, $b_z=0$, and $b_v=1$.

VII. AXIAL CURRENT

The steady-state axial current is modified by the finite-amplitude oscillations. Because of the phase difference between the density and potential oscillations, we get contributions to $\Gamma_\pm$ from terms of the type $n\mathbf{E}$ when these are time averaged. For the z component we obtain

$$\langle nE_z \rangle_{av} = N_0 h_0 E_{z0} + \tfrac{1}{2} N_1 U_1 k f g \sin\delta.$$

Using Eqs. (3), we derive

$$\langle \Gamma_{+z} \rangle_{av} - \langle \Gamma_{-z} \rangle_{av} = \frac{N_0(\mu_- + \mu_+)(V_- + V_+)}{R}$$

$$\times \left[\left(h_0 + \eta_1 + \eta_2 \frac{\gamma_3}{\gamma_5} \right) \left(\frac{E_{z0}R}{V_- + V_+} \right) + \frac{2\pi R \phi f g}{m\lambda\gamma_5\sqrt{y}} \right],$$

where $\lambda = 2\pi/k$. It can be shown from Eq. (25) that when the instability develops, we require that k and E_{z0} have opposite sign. Thus, the presence of the helix tends to decrease the axial current, while increasing the current in the azimuthal direction.

We obtain the total axial current through the sample by integrating over the cross section of the sample. The result is

$$I_t = \frac{2\pi e(\mu_+\mu_-)^{1/2}\gamma_5 N_0(V_- + V_+)}{R}$$

$$\times \left[\left(\frac{E_{z0}R}{V_- + V_+} \right) \int_0^R r \left(h_0 + \eta_1 + \eta_2 \frac{\gamma_3}{\gamma_5} \right) h_0 dr \right.$$

$$\left. - \frac{2\pi\phi}{m\gamma_5(\lambda/R)\sqrt{y}} \int_0^R \frac{r J_m^2(\beta_1 r)}{h_0 + \gamma} dr \right], \quad (30)$$

where e is the electron charge.

VIII. ENERGY BALANCE OF SEMICONDUCTOR PLASMAS

The results obtained for the finite-amplitude helical-mode theory have been achieved in a self-consistent manner. As they are presented, they are, however, not in a form readily applicable to experimental observations. The computed dimensionless electric field, frequency, and magnetic field depend on the temperatures $V_\pm$ and the mobilities $\mu_\pm$. Furthermore, the argument $\beta_0 R$, for which the zero-harmonic radial density distribution equals zero, is related to the ionization rates $\xi_\pm$ and the recombination time τ.

Generally, the variables which are observed experimentally are the axial-vector electric field E_{z0} and the frequency ω_r of the oscillation as a function of the applied axial-vector magnetic field B_0. The current is

usually kept constant as the magnetic field is changed. The thermal background densities $n_\pm$ are determined from conductivity measurements.

A knowledge of the dependence of the parameters described above as a function of the electric field is a prerequisite to further analysis. With an application to n-InSb in mind, we therefore, present the results of energy-balance calculations for polar semiconductors with hyperbolic band structures.

For a semiconductor with a hyperbolic band structure, the electron energy ϵ is given in terms of the momentum $\mathbf{p}$ by

$$\epsilon_\mathbf{p} = \Delta(1 + \mathbf{p}^2/em\Delta)^{1/2},$$

where $\Delta = \tfrac{1}{2}V_i$ is half the forbidden band width V_i and m is the effective electron mass.

We consider collisions between electrons and optical phonons to be the main collision process. Taking account of emission and absorption of phonons with wave vectors $\mathbf{q}/\hbar$, we define the mean time $\tau_{ph}(\epsilon)$ between collisions of electrons with energy ϵ and phonons as[26]

$$\frac{1}{\tau_{ph}(\epsilon)} = \frac{V_c}{2\pi\hbar^4} \left(\int_{qa1}^{qau} \int_{-1}^{1} G(q)N_q \right.$$

$$\times \delta(\epsilon_{\mathbf{p}+\mathbf{q}} - \epsilon_\mathbf{p} - \hbar\omega_0)q^2 d(\cos\chi)dq$$

$$+ \int_{qe1}^{qeu} \int_{-1}^{1} G(q)(N_q + 1)$$

$$\left. \times \delta(\epsilon_{\mathbf{p}-\mathbf{q}} - \epsilon_\mathbf{p} + \hbar\omega_0)q^2 d(\cos\chi)dq \right), \quad (31)$$

where the first term is due to absorption and the second to emission of phonons. N_q is the equilibrium number of phonons:

$$N_q = (e^{2\beta} - 1)^{-1},$$

where $\beta = V_{op}/2V_0$; V_{op} is the optical phonon temperature, V_0 is the lattice temperature, and $\hbar\omega_0$ is the energy of optical phonons with frequency ω_0. $G(q)$ is the square of the interaction matrix element, and, for interaction with polar optical vibrations, Frøhlich[27] has shown that

$$G(q) = \frac{2\pi e^2 \hbar^2 \hbar\omega_0}{V_c q^2} \left(\frac{1}{\epsilon_\infty} - \frac{1}{\epsilon_s} \right),$$

where V_c is the volume of the crystal, and ϵ_∞ and ϵ_s are the high-frequency and static permittivities, respectively; χ is the angle between $\mathbf{p}$ and $\mathbf{q}$.

Integration over the angle χ removes the δ functions in Eq. (31). The upper and lower limits on the integra-

[26] R. Stratton, *Progress in Dielectrics* (Heywood and Co. Ltd., London, 1961), Vol. 3, p. 233.

[27] H. Frøhlich. Advan. Phys. 3, 325 (1954).

tions over q are determined for $\cos\chi=\pm 1$ and are

$$\left.\begin{array}{c}q_{au}\\q_{al}\end{array}\right\}=\hbar^{-1}(me\Delta)^{1/2}$$

$$\times\{\pm[(\epsilon/\Delta)^2-1]^{1/2}+[(\epsilon+\hbar\omega_0)^2/\Delta^2-1]^{1/2}\},$$

$$\left.\begin{array}{c}q_{eu}\\q_{el}\end{array}\right\}=\hbar^{-1}(me\Delta)^{1/2}$$

$$\times\{[(\epsilon/\Delta)^2-1]^{1/2}\pm[(\epsilon-\hbar\omega_0)^2/\Delta^2-1]^{1/2}\}.$$

The mean free path $l_{ph}(\epsilon)$ is given by $l_{ph}=v\tau_{ph}$, where the electron velocity is given by

$$v=e\frac{d\epsilon}{dp}=\left(\frac{e}{m}\Delta\right)^{1/2}\frac{\Delta}{\epsilon}[(\epsilon/\Delta)^2-1]^{1/2}.$$

For energies $\Delta<\epsilon<\Delta+\hbar\omega_0$ only absorption of optical phonons is permitted, and for this case the mean free path is

$$l_{ph}^{-1}=l_0^{-1}\frac{\epsilon^2\hbar\omega_0}{\Delta^3}\frac{1+\hbar\omega_0/\epsilon}{(\epsilon/\Delta)^2-1}\frac{2}{\exp(2\beta)-1}$$

$$\times\ln\frac{[(\epsilon/\Delta)^2-1]^{1/2}+[(\epsilon+\hbar\omega_0)^2/\Delta^2-1]^{1/2}}{[(2\epsilon+\hbar\omega_0)\hbar\omega_0/\Delta^2]^{1/2}},\quad(32)$$

where l_0 has the dimension of length and is given by

$$l_0^{-1}=\frac{e^2m}{\hbar^2}\left(\frac{1}{\epsilon_\infty}-\frac{1}{\epsilon_s}\right).\quad(33)$$

For energies $\epsilon>\Delta+\hbar\omega_0$ both absorption and emission of phonons must be included, and

$$l_{ph}^{-1}=l_0^{-1}\frac{\epsilon^2\hbar\omega_0}{\Delta^3}\frac{1+\hbar\omega_0/\epsilon}{(\epsilon/\Delta)^2-1}\frac{2}{e^{2\beta}-1}$$

$$\times\left[\ln\frac{[(\epsilon/\Delta)^2-1]^{1/2}+[(\epsilon+\hbar\omega_0)^2/\Delta^2-1]^{1/2}}{[(2\epsilon+\hbar\omega_0)\hbar\omega_0/\Delta^2]^{1/2}}\right.$$

$$\left.+e^{2\beta}\frac{\epsilon-\hbar\omega_0}{\epsilon+\hbar\omega_0}\ln\frac{[(\epsilon/\Delta)^2-1]^{1/2}+[(\epsilon-\hbar\omega_0)^2/\Delta^2-1]^{1/2}}{[(2\epsilon-\hbar\omega_0)\hbar\omega_0/\Delta^2]^{1/2}}\right].$$

$$(34)$$

We use these expressions for the mean free path due to scattering on phonons in the following calculations.

In order to calculate the electron temperature and mobility, and the ionization rate, it is necessary to know the electron-velocity distribution function. In particular, for the calculation of the ionization rate, one has to compute the high-energy non-Maxwellian tail of this distribution. An analysis of this kind has been given by Keldysh[24] for nonpolar semiconductors and has been extended to polar semiconductors by Chuenkov.[25] Below we present a short synopsis of the Chuenkov theory.

The basic assumptions which are employed are that the solid-state plasma is in thermal equilibrium with the lattice and that the plasma is in a steady-state homogeneous condition. The principal energy losses which are considered are collisions of electrons with optical phonons. The energy of the plasma lost by impact ionization and by collisions with acoustical phonons are neglected. The energy is supplied to the electrons by the applied electric field. The excess electrons created by the process of impact ionization are considered small, so that an equilibrium density can be approximated.

Chuenkov calculates an explicit expression for the impact-ionization coefficient for polar semiconductors. For this derivation, he first calculates the complete electron-distribution function by looking for a solution of the electron-transport equation in the form

$$f(\mathbf{p})=C\sum_{n=0}^{\infty}\phi_n(\epsilon)P_n(\cos\theta)\exp\left(-\int_\Delta^\epsilon\frac{s(\epsilon')d\epsilon'}{eE_{z0}l(\epsilon')}\right),\quad(35)$$

where $\phi_n(\epsilon)$ are energy-dependent coefficients, C is a constant, θ is the angle between the electric field and the momentum, and $s(\epsilon)$ is a function of energy to be determined. By treating $\phi_n(\epsilon)$ as weakly dependent on energy compared to the exponential and then integrating the transport equation over all angles to determine the symmetric part of the distribution function, we obtain

$$f_0(\epsilon)=\frac{1}{2}\int_{-1}^{+1}f(\mathbf{p})d(\cos\theta)$$

$$=C\exp\left(-\int_\Delta^\epsilon\frac{s(\epsilon')d\epsilon'}{eE_{z0}l(\epsilon')}\right),\quad(36)$$

where the function $s(\epsilon)$ is determined by the transcendental equation

$$2s\ln[2(\epsilon^2-\Delta^2)/\epsilon\hbar\omega_0]\cosh\beta/\cosh(\beta-\alpha s)=\ln\frac{1+s-\{1-1/\ln[2(\epsilon^2-\Delta^2)/\epsilon\hbar\omega_0]\}\cosh(\beta-\alpha s)/\cosh\beta}{1-s-\{1-1/\ln[2(\epsilon^2-\Delta^2)/\epsilon\hbar\omega_0]\}\cosh(\beta-\alpha s)/\cosh\beta},\quad(37)$$

where we defined the quantity $\alpha(\epsilon)=\hbar\omega_0/eE_{z0}l(\epsilon)$. We note that, by combining equations (32), (34), (36), and (37) we can determine the distribution function

$f_0(\epsilon)$ as a function of energy for fixed values of the applied electric field and the lattice temperature.

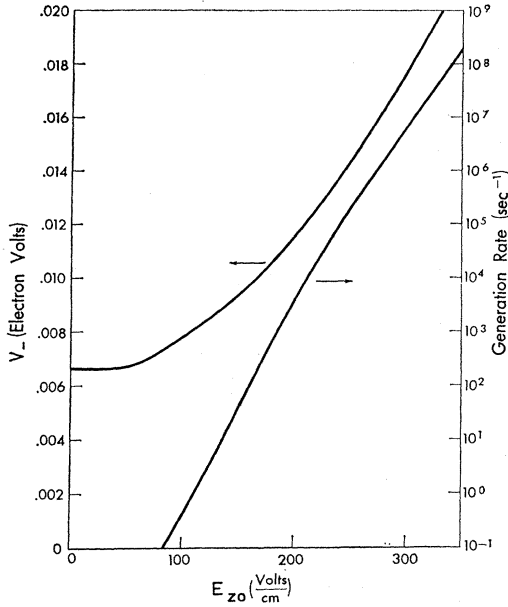Using this expression for the symmetric part of the

FIG. 7. Electron temperature V_- and the ionization rate ξ_- as functions of the electric field for n-InSb.

distribution function, Chuenkov calculates the ionization rate ξ_- to be

$$\xi_-(E_{z0},V_0)=\int_{V_i+\Delta}^{\infty}\tau_i^{-1}(\epsilon)f_0(\epsilon)\epsilon\left[\left(\frac{\epsilon}{\Delta}\right)^2-1\right]^{1/2}d\epsilon\Big/$$

$$\int_{\Delta}^{\infty}f_0(\epsilon)\epsilon\left[\left(\frac{\epsilon}{\Delta}\right)^2-1\right]^{1/2}d\epsilon,\quad(38)$$

where the impact ionization probability $\tau_i^{-1}(\epsilon)$ for $\epsilon-V_i\ll V_i$ is given by

$$\tau_i^{-1}(\epsilon)=\tau_{\mathrm{ph}}^{-1}(V_i)p_0\left(\frac{\epsilon-V_i}{V_i}\right)^j,\quad(39)$$

where p_0 is a dimensionless constant and j can assume the values 1, 2, or 3, depending on the structure of the crystal and its permittivity. The complete distribution function is given by Chuenkov as

$$f(\mathbf{p})=\frac{A'}{B'-s\cos\theta}f_0(\epsilon),\quad(40)$$

where for simplicity we have introduced

$$A'=\frac{\cosh(\beta-\alpha s)}{(\cosh\beta\ \ln[2(\epsilon^2-\Delta^2)/\epsilon\hbar\omega_0])},$$

$$B'=1-\left(1-\frac{1}{\ln[2(\epsilon^2-\Delta^2)/\epsilon\hbar\omega_0]}\right)\frac{\cosh(\beta-\alpha s)}{\cosh\beta}.$$

The electron mobility is obtained from the drift velocity $v_d=\mu_-E_{z0}$ given by

$$v_d=\int v(\mathbf{p})\ \cos\theta f(\mathbf{p})d^3p\Big/\int f(\mathbf{p})d^3p.$$

After performing the integration over the angles and expressing the result in terms of an integral over the energy, we obtain

$$\mu_-=\frac{1}{E_{z0}}\left(\frac{\Delta}{m}\right)^{1/2}$$

$$\times\int_\Delta^\infty\left[\left(\frac{\epsilon}{\Delta}\right)^2-1\right]\frac{\Delta}{s}A'\left(2+\frac{B'}{s}\ln\frac{B'-s}{B'+s}\right)f_0(\epsilon)d\epsilon\Big/$$

$$\int_\Delta^\infty\left[\left(\frac{\epsilon}{\Delta}\right)^2-1\right]^{1/2}\frac{\epsilon}{s}A'\ln\frac{B'-s}{B'+s}f_0(\epsilon)d\epsilon,\quad(41)$$

where all the energy dependences are known. In order to adjust the zero-field mobility to particular values in different semiconductor specimens, we use the constant l_0, which enters into the equation for $s(\epsilon)$ as an adjustable parameter.

An "effective" electron temperature V_- is obtained by averaging over the electron energy,

$$V_-=\tfrac{2}{3}\langle\epsilon-\Delta\rangle_{\mathrm{av}}$$

$$=\tfrac{2}{3}\Delta\int_\Delta^\infty\frac{\epsilon}{\Delta}\left(\frac{\epsilon}{\Delta}-1\right)\left[\left(\frac{\epsilon}{\Delta}\right)^2-1\right]^{1/2}f_0(\epsilon)d\epsilon\Big/$$

$$\int_\Delta^\infty\frac{\epsilon}{\Delta}\left[\left(\frac{\epsilon}{\Delta}\right)^2-1\right]^{1/2}f_0(\epsilon)d\epsilon.\quad(42)$$

By specifying the values for the longitudinal electric field and the lattice temperature, we thus calculate the effective electron temperature, the electron mobility, and the ionization rate. Some uncertainty is connected with the corresponding parameters for the holes. For the purpose of our present numerical calculations we have related the electron and hole quantities by the simple relations given in Sec. IX.

In Fig. 7 we have plotted the electron temperature and the ionization rate as functions of the electric field at a lattice temperature of 77°K. For $E_{z0}\sim300$ V/cm the value of ξ_- is compatible with those observed.[28,29] The range of ξ_- values for which the wall losses balance the ionization in the bulk can be estimated from the definition of β_0R in Table I. With $\xi_-\gg\xi_+$, $1/\tau$ and $y\ll1$ we have

$$\xi_-\approx\frac{\mu_-(V_-+V_+)}{(b+1)R^2}(\beta_0R)^2.$$

[28] J. C. McGroddy and M. I. Nathan, J. Phys. Soc. Japan Suppl. **21**, 437 (1966).
[29] D. K. Ferry and H. Heinrich, Phys. Rev. **169**, 670 (1968).

With a value $\beta_0 R \sim 1.5$ taken from Fig. 2, and the other parameters as specified below, we obtain $\xi_- \sim 1.5 \times 10^5$ sec^{-1}. In our case this corresponds to an electric field $E_{z0} \sim 240$ V/cm. This value seems somewhat high in view of the results of McGroddy and Nathan,[28] which indicate breakdown at this value.

The longitudinal current given by Eq. (30) is calculated in the absence of an instability ($\phi = 0$) as a function of the electric field, and the result is shown in Fig. 8.

IX. NUMERICAL RESULTS

In order to present our results in terms of quantities which are directly measurable, we seek numerical solutions in which the electric field E_{z0}, the frequency f-$\omega_r/2\pi$, and the wavelength λ are computed as functions of the magnetic field B_0, under the condition that the current is constant. In order to do this, a definite semiconductor specimen must be specified. The modification of the Keldysh theory[24] presented by Chuenkov[25] is directly applicable to n-type indium antimonide with the numerical constants $p_0 = 100$ and $j = 2$. Furthermore, we have $V_{op} = 2.44 \times 10^{-2}$ eV, $V_i = 0.22$ eV, and a lattice temperature $V_0 = 6.6 \times 10^{-3}$ eV. For the electron mass we use $m_- = 0.016\, m_0$, where m_0 is the free electron mass. As a typical low-field electron mobility we take $\mu_{-0} = 50$-m^2/Vsec and use a constant mobility ratio $\mu_-/\mu_+ = 62.5$. The electron and hole temperatures are assumed to be equal and $\xi_- \gg \xi_+$, $1/\tau$. The value of R is determined by the sample size and is typically 4×10^{-4} m. For the background density n_- we use the value $n_- = 10^{19}$ m^{-3}, which yields currents for which the theory is most likely to apply.
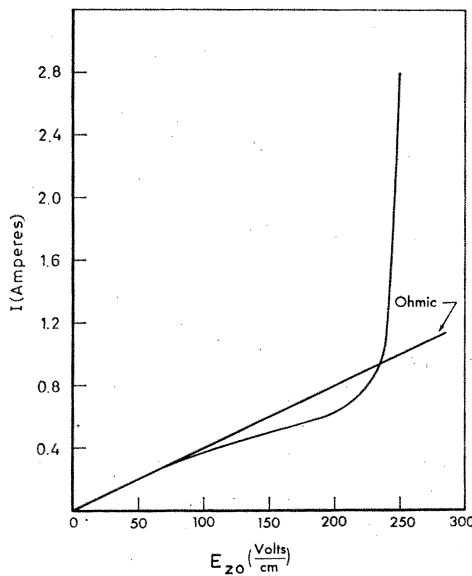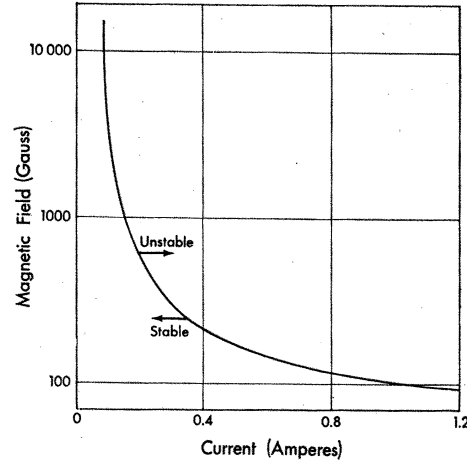

FIG. 9. Critical magnetic field for the onset of the helical instability as a function of the current through the semiconductor.

We will give an example of the numerical analysis used to obtain solutions for n-type InSb. The onset of the helical instability was the first criterion to be determined. The value of n_-/N_0 was fixed and a value for y was chosen. Equation (13) was then solved numerically for $\phi = 0$. This provided the radial dependence of $h_0(r)$ and also determined $\beta_{00}R$. Knowing these values, we were then able to determine the value of $E_{z0}R/(V_-+V_+)$ for the chosen value of y. From the energy-balance calculations, with the same values of y and $\beta_{00}R$, it was possible to determine another value of $E_{z0}R/(V_-+V_+)$. This process was then repeated as the value of y was changed until the value of $E_{z0}R/(V_-+V_+)$ was identical in both the helical-instability calculations and in the energy-balance calculations. It was then possible to determine the value of the current which corresponds to this particular value of n_-/N_0. The value of n_-/N_0 was changed and a new critical magnetic field was obtained for another value of the current. As a result it was possible to determine the critical magnetic field for the onset of the helical instability as a function of the current through the semiconductor, as shown in Fig. 9. We now treat the problem of the finite-amplitude helix. A value of the current is chosen from the preceding calculations for determining the onset of the helical instability. A value for $\beta_0 R$ is then fixed which is somewhat greater than the value $\beta_{00}R$ obtained from the perturbation analysis. Values for n_-/N_0, y, and ψ are then specified. Knowing these values, we are then able to determine h_0 and ϕ from Eq. (13). When we use these values of $\beta_0 R$, n_-/N_0, y, h_0, and ϕ, it is then possible to determine a value of ψ from Eq. (23). This value of ψ is used in Eq. (13), keeping the other parameters fixed. Then new values for h_0 and ϕ are obtained. This process is repeated until ψ converges. The value of $E_{z0}R/(V_-+V_+)$ corresponding to the convergent value of ψ is determined and compared to the value determined from the energy-balance calculations. The

FIG. 8. Voltage current characteristic of n-InSb as calculated from the theory of impact ionization in semiconductors.
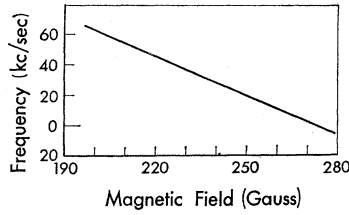
FIG. 10. Frequency of the finite-amplitude helix as a function of the applied magnetic field for n-InSb.

value of y is then adjusted until the values of $E_{z0}R/(V_-+V_+)$ from both calculations are nearly identical. The current is then calculated and compared to its value for $\phi=0$. Finally, the value of n_-/N_0 is adjusted and all the preceding calculations repeated until the current obtained for this fixed value of $\beta_0 R$ is the same as that obtained at $\phi=0$. The parameters describing the helix are then calculated for this value of the magnetic field. A number of values for $\beta_0 R$ are taken so that a range of magnetic fields can be analyzed at a fixed current. The results of these calculations are shown in Fig. 10, where we plot the frequency of the helix as a function of the applied magnetic field for a fixed total current $I_t=0.44$ A. The wavelength of the helix as a function of the applied magnetic field is shown in Fig. 11 for the same value of the current.

The results shown in Figs. 9–11 are based on the complementation of two different theories. The finite-amplitude helical-mode theory is essentially the one which determines the shape of the curves. The semiconductor impact ionization and energy-balance theory determines the position of the curves in the plot. To avoid some of the uncertainties in the latter theory, it is thus preferable to give the final results independent of E_{z0}, which is the most uncertain parameter.

X. CONCLUSION

The helical instability of a finite amplitude has been investigated for solid-state electron-hole plasmas. Plasma density profiles were obtained in the absence of an instability as a function of the ratio of the thermal carriers to the plasma density along the axis. Changes in the plasma density profiles were then calculated as a function of the amplitude of the helical instability. For
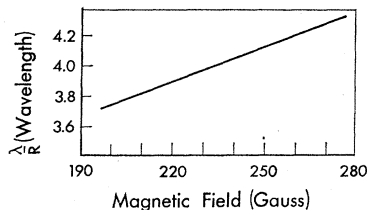

FIG. 11. Wavelength of the finite-amplitude helix as a function of the applied magnetic field for n-InSb.

a given value of the amplitude of the helical instability, the wavelength which was most unstable as the electric field increased was calculated. This determined the value of the ratio between the electric field and the electron temperature, necessary for the condition of marginal stability. This also determined the corresponding value for the frequency of the helix. These results were then combined with the energy-balance theory for the solid-state electron-hole plasma to obtain values which could be compared directly with experiments. It was found that, for n-InSb with a constant current flowing, the wavelength of the helix increased with increasing magnetic field while the frequency decreased to zero, changed sign, and then increased with an increasing magnetic field.

APPENDIX

Several assumptions are made which limit the range of applicability of the present theory. Below we summarize the more important assumptions and their relevance to possible experiments.

(1) The azimuthal magnetic field B_θ has been neglected. As indicated by the onset of pinch effects, this approximation can not hold above certain currents.[30] For the B_θ field to be negligible it must be so small that it does not significantly alter the radial flow of particles.

From Eqs. (3) we compute the radial flow vector components $\Gamma_{\pm r}$. Since $\Gamma_{-r}=\Gamma_{+r}=\Gamma_r$, we obtain

$$\Gamma_r = -\frac{\mu_-(V_-+V_+)}{(1+y)(b+1)}\left(1+\frac{C_1}{h_0+\gamma}\right)$$
$$\times\left(\frac{dn}{dr}+\frac{N_+N_-}{n_+V_-+n_-V_++(V_-+V_+)n}(\mu_-+\mu_+)B_\theta E_{z0}\right). \tag{A1}$$

Thus B_θ is negligible when

$$\left|\frac{dn}{dr}\right|\gg\frac{N_+N_-}{n_+V_-+n_-V_++(V_-+V_+)n}(\mu_-+\mu_+)B_\theta E_{z0}. \tag{A2}$$

By considering the limit $n\gg n_\pm$, a simpler version of (A1), correct within a factor of ~ 2, can be derived. In the stationary unperturbed state, n is given by a zero-order Bessel function, i.e., $n=N_0 J_0(\beta_0 r)$.

We obtain

$$e\mu_0(\mu_-+\mu_+)^2\frac{V_-+V_+}{(\beta_0 R)^2}\left(\frac{E_{z0}R}{V_-+V_+}\right)^2 N_0 J_0(\beta_0 r)\ll 1, \tag{A3}$$

where μ_0 is the permeability of the material.

[30] K. Ando and M. Glicksman, Phys. Rev. **154**, 316 (1967).

An alternative version of Eq. (A2) in terms of the axial current is

$$I_t \ll \frac{4\pi}{\mu_0} \frac{V}{E_{z0}(\mu_- + \mu_+)}, \qquad (A4)$$

where

$$V = V_-, \quad n\text{-type material,}$$
$$= V_+, \quad p\text{-type material.}$$

In deriving Eq. (A4), we have put $|dn/dr| = N_0/R$ and used the maximum of the last term in (A1).

For n-InSb with $E_{z0} \sim 10^4$ V/m we roughly take $V_- = V_{\mathrm{op}}$ and $\mu_- = \frac{1}{2}\mu_{-0}$ and obtain $I_t \ll 1A$.

(2) We have used the boundary condition $h_0(R) = 0$, based on an infinite surface recombination velocity s_R at the surface $r = R$. In experiments, special precautions should be taken to prepare the surface of the specimens in order to make this approximation valid. In order to have $h_0(R) \ll 1$, we require

$$s_R \gg \tfrac{1}{2}\mu_-(V_- + V_+)$$

$$\times \frac{(\beta_0 R)^2}{(1+y)(b+1)R}\left(\frac{2}{R^2}\int_0^R rh_0 dr + \gamma_z\right), \quad (A5)$$

where we have used the integrated Eq. (14),

$$R\left(1 + \frac{C_1}{h_0 + \gamma}\right)\frac{dh_0}{dr}\bigg|_{r=R} = -\beta_0^2 \int_0^R rh_0 dr - \tfrac{1}{2}\gamma_z(\beta_0 R)^2, \quad (A6)$$

together with the condition $\Gamma_r(R) = N_0 h_0(R)s_R$, where Γ_r is given by Eq. (A1) with $B_\theta = 0$.

For n-type material, $\beta_0 R \sim 2$, and in Eq. (A5) the first term in the bracket is $\sim\frac{1}{2}$. With the previous material specifications for InSb we get $s_R \gg 50$ m/sec, or, for small injection levels when γ_z becomes large, $s_R \gg 50 \times n_-/N_0$ m/sec.

(3) For a constant steady-state density along the axis, it is necessary that the main plasma production process is impact ionization in the bulk rather than injection at the ends. We consider Eq. (A6) which, together with Eq. (A1), yields

$$\Gamma_r(R) = \frac{\mu_-(V_- + V_+)}{(1+y)(b+1)R}\left(\beta_0^2\int_0^R rh_0 dr + \tfrac{1}{2}\gamma_z(\beta_0 R)^2\right). \quad (A7)$$

For outward or zero flow at the surface $r = R$, $\Gamma_r(R) \geq 0$, and thus, by using Table I, we obtain

$$\left(2\pi N_0 \int_0^R rh_0 dr + \pi R^2 n_0\right)\xi_-$$

$$+ \left(2\pi N_0 \int_0^R rh_0 dr + \pi R^2 p_0\right)\xi_+ \geq 2\pi\frac{N_0}{\tau}\int_0^R rh_0 dr \quad (A8)$$

as a condition to be fulfilled in order to have no z variation in the steady state. In particular, for n-type material with $\xi_- \gg \xi_+$,

$$\xi_- \geq \frac{1}{\tau}\left[1 + \left(\pi R^2 \Big/ 2\pi\int_0^R rh_0 dr\right)\frac{n_-}{N_0}\right]^{-1}. \quad (A9)$$

We note that this condition for low injection levels is rather weak, i.e., $\xi_- \gtrsim N_0/2n_-\tau$, while for high injection levels it is $\xi_- \geq 1/\tau$. In the numerical calculations we have put $\tau = \infty$.

(4) We have not considered the effect of the magnetic field on the ionization rate. At the relatively small magnetic fields for which the helical instability may be excited ($B_0 \lesssim 500$ G), the results of Ferry and Heinrich[29] indicate that the magnetic field does not significantly change the ionization rate.